

RETAILOPT: An Opt-In, Easy-to-Deploy Trajectory Estimation System Leveraging Smartphone Motion Data and Retail Facility Information

RYO YONETANI and JUN BABA, CyberAgent, Japan

YASUTAKA FURUKAWA, Simon Fraser University, Canada

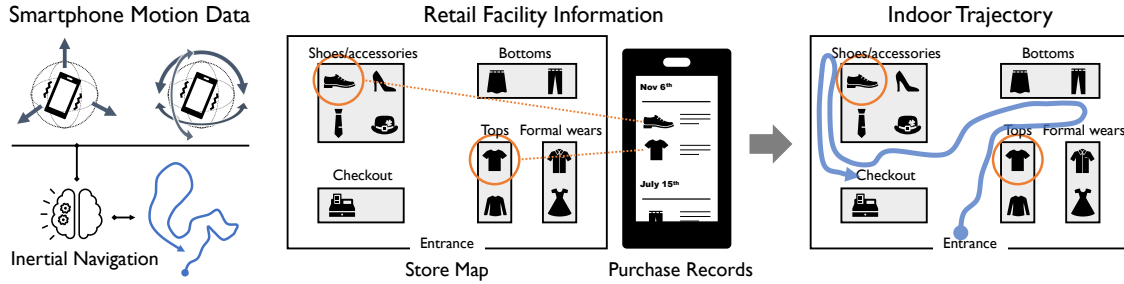


Fig. 1. The **RETAILOPT** System leverages smartphone motion data, store map, and purchase records to enable opt-in, easy-to-deploy indoor trajectory estimation in retail environments.

We present **RETAILOPT**, a novel opt-in, easy-to-deploy system for tracking customer movements in indoor retail environments. The system utilizes information presently accessible to customers through smartphones and retail apps: motion data, store map, and purchase records. The approach eliminates the need for additional hardware installations/maintenance and ensures customers maintain full control of their data. Specifically, **RETAILOPT** first employs inertial navigation to recover relative trajectories from smartphone motion data. The store map and purchase records are then cross-referenced to identify a list of visited shelves, providing anchors to localize the relative trajectories in a store through continuous and discrete optimization. We demonstrate the effectiveness of our system through systematic experiments in five diverse environments. The proposed system, if successful, would produce accurate customer movement data, essential for a broad range of retail applications, including customer behavior analysis and in-store navigation. The potential application could also extend to other domains such as entertainment and assistive technologies.

CCS Concepts: • **Human-centered computing** → **Ubiquitous and mobile computing systems and tools**.

Additional Key Words and Phrases: Indoor localization; Inertial navigation; Neural networks

1 INTRODUCTION

Imagine owning a fashion store. You would know the locations of entrances, walls, and shelves, and what items are displayed on which shelves. The purchase records from the points-of-sales (POS) cash registers reveal which customer purchased which items. Such granular retail facility information provides rich constraints for tracking the movement of every customer, holding significant potential for retail applications such as targeted marketing [17, 45, 65], improved in-store navigation [30, 54, 56], inventory management [8], and anomalous behavior detection [2, 49, 60]. Technologies that capture the trajectories of people in indoor environments could impact broader domains beyond the retail industry, for example, enhancing visitor experiences in museum or theme parks [37] and assistive navigation technologies [53].

Location-based services should require minimal additional costs and employ an opt-in mechanism to respect customer privacy. Existing indoor global positioning systems (GPS) or motion-tracking approaches require an expensive site

Authors' addresses: Ryo Yonetani, yonetani_ryo@cyberagent.co.jp; Jun Baba, baba_jun@cyberagent.co.jp, CyberAgent, 40-1 Utagawa-cho, Shibuya-ku, Tokyo, Japan, 150-0042; Yasutaka Furukawa, furukawa@sfu.ca, Simon Fraser University, 8888 University Drive, Burnaby, BC, Canada, V5A 1S6.

survey to collect referential environmental information, such as geo-localized visual features [43, 51, 55, 63, 75, 81], wireless fingerprints [14, 24, 29, 52, 69, 80, 91, 92], or magnetometer responses [42, 87], at every location within the environment in advance. The collected information further requires maintenance upon environmental changes. Active installation of hardware components, such as ultra-wideband (UWB) systems [59] or surveillance cameras [6, 16, 26, 76], can achieve high precision and is more resilient to environmental changes, but the hardware installation beyond existing infrastructure incurs significant costs to building/store owners.

This paper proposes RETAILOPT, a novel system for tracking customer movements in indoor retail environments (See Fig. 1). Our system fuses two information sources: the smartphone motion data and retail facility information. Inertial navigation recovers a relative motion trajectory of each customer from inertial measurement unit (IMU) sensor data [89]. Retail facility information, specifically *store maps and purchase records*, identify *anchors* that indicate global reference positions and help localize the relative trajectory in a store. The store map provides the physical layout (*i.e.*, locations of shelves, corridors, doors, *etc.*) and the semantic layout (*i.e.*, “which items are on which shelves.”) The purchase records (*i.e.*, “which items were purchased”) reveal which shelves were visited, thereby serving as anchors that reference their locations. The main technical challenge is how to align relative trajectories with the anchors *without knowing when they were visited*. As shown in Fig. 2, we develop a novel continuous-discrete optimization pipeline, where the relative trajectories are first matched to time-unknown anchors via gradient descent and projected onto the non-obstacle space based on the Viterbi algorithm.

The RETAILOPT system requires minimal additional costs for hardware installation and maintenance. Modern smartphones are equipped with IMUs that are easily accessible from third-party apps with permission from users. Arguably, a large number of people use retailer’s smartphone apps to access store information, check sale items, or earn reward points [31, 48, 77, 85]. Recent apps provide customer’s purchase histories as well as in-store maps.¹ Such facility information is kept up-to-date in retailer’s daily operations, thus minimizing maintenance costs compared to systems based on popular wireless fingerprinting. Furthermore, our system enables customer tracking through opt-in consent. Unlike visual tracking and other passive localization techniques, we estimate trajectories using data from customers’ smartphones, ensuring customers have full control over their data.

We evaluate the localization accuracy in five environments. We have collected IMU sensor data and ground-truth positions from 15 participants moving around retail stores and visiting shelves while holding a smartphone naturally in a hand, pocket, or bag.² The proposed system archives the average positional error of less than approximately 3 meters, considerably lower than baseline methods [18, 23, 89]. It also outperforms the baselines as well as a state-of-the-art inertial localization method [21] in larger environments (*i.e.*, trajectories longer than 400 meters) such as office spaces or university campuses.

2 RELATED WORK

Trajectory estimation for pedestrians in indoor environments has been a popular research topic in many fields, including computer vision, robotics, human-computer interaction, and ubiquitous computing. Existing techniques employ combinations of different modalities (*e.g.*, wireless technologies, cameras, or IMUs) and methodologies (*e.g.*, location fingerprinting, triangulation, or motion tracking, sometimes combined with machine learning). This section reviews recent studies that specifically utilizes IMUs and simultaneous localization and mapping (SLAM), along with some relevant techniques that aid in aligning trajectories with referential localization anchors. For a more comprehensive

¹Walmart app is a good example: <https://www.walmart.com/cp/find-an-item-store-maps/6422847>.

²Our experiments passed the ethics review board of the author’s affiliation to publish the collected data for research purposes.

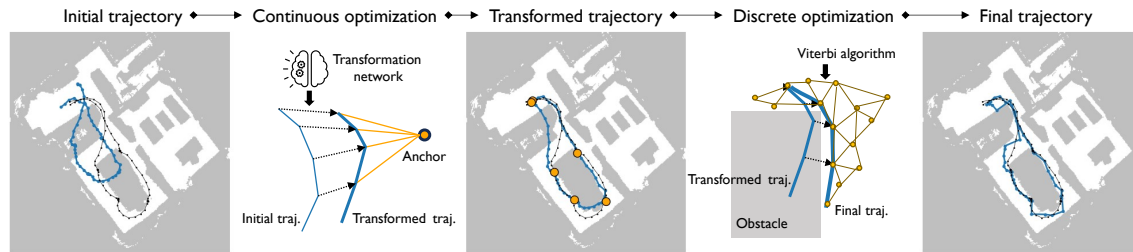


Fig. 2. **Trajectory Estimation Pipeline.** Given a relative motion trajectory obtained from inertial navigation (blue lines in the figure, while ground-truth trajectories obtained by visual-inertial SLAM is shown in black lines), we first transform it to better align with localization anchors (orange circles) identified by cross-referencing the store map and customer’s purchase records. This is achieved by optimizing a transformation network via gradient descent with back-propagation. The transformed trajectory is further projected onto the valid space using a Viterbi algorithm, ensuring the final trajectory does not collide with obstacles in the environment.

understanding of other methods, such as location fingerprinting using wireless signals and visual surveillance utilizing cameras, readers are referred to the following surveys: [1, 26, 52, 55, 80, 86, 91].

Tracking People using IMUs. Inertial navigation and pedestrian dead reckoning (PDR) utilize acceleration and angular velocity measurements from IMUs to estimate the relative positions of subjects, that is, positions relative to the initial position [25, 86]. IMUs suffer from complex sensor noise, particularly during motions, where analytical solutions are infeasible [90]. Supervised machine learning has been successful instead, which collects pairs of IMU data and motion trajectories and learns a mapping function between them, often by a neural network model. The robust neural inertial navigation (RoNIN) system [89] is a landmark study that employs deep neural networks to enhance performances in challenging real-world scenarios. Neural inertial odometry combines neural network predictions with existing odometry systems, while assuming that IMUs are rigidly attached to the body [44, 61, 70]. Some recent work also seeks to improve network architectures and learning algorithms to tackle the domain shift problem [7, 10]. Building on these advancements, our focus is on how to geo-localize such relative trajectories from inertial navigation within the environment, aided by information from retail facilities. Neural inertial localization [21] is one of the most recent machine learning-based attempts to localize positions solely from IMU data.

Localization using Anchors. Our system utilizes retail facility information to form anchors, *i.e.*, referential landmarks with known global positions in a map, with which relative trajectories from inertial navigation are geo-localized. Such anchors can be constructed by dedicated devices [8, 11, 19, 22, 35, 41, 47, 79, 93], other people’s smartphones [12], or environmental features such as acoustic signals [73] or motion signals induced by the environment [56, 82]. Our anchors are constructed with environmental features, eliminating the need for additional device installation. Furthermore, the retail facility information remains updated during routine operations without requiring extra site surveys.

Trajectory Alignment. Techniques to align trajectories with global referential cues have also been explored in other fields. For instance, map matching, a technique in intelligent transportation systems and mobile robotics, aligns the trajectories of moving agents (*e.g.*, vehicles, robots) with road networks [46]. For comprehensive reviews, see [20, 57] for classical surveys and [27, 68] for more recent works. Another relevant technique is point-set registration, studied in 3D computer vision and robotics, which calculates a transformation between a pair of unordered point sets [72]. Popular methods include iterative closest point (ICP) algorithms [3, 66, 84] that alternately identify point-to-point

Table 1. **Solution-Level Comparisons for Indoor Trajectory Estimation.** Compared to other possible solutions like wireless localization and visual surveillance systems, RETAILOPT requires minimum costs for additional hardware installation and operations on the retailer’s side, and employs opt-in/out mechanisms.

Solutions	Additional hardware	Additional operations	Opt-in/out
Wireless localization Inertial navigation w/ wireless anchors	Anchor devices	Regular site surveys	Supported
Visual surveillance	Cameras	N/A	Not supported
RETAILOPT (Inertial navigation w/ retail facility info.)	N/A (Customer’s smartphones)	N/A (Maintenance of facility info.)	Supported

correspondences and rigid transformations between them. Also, the coherent point drift (CPD) algorithms [18, 23, 50] can identify coherent, non-rigid transformations between point sets within a probabilistic framework.

Simultaneous Localization and Mapping (SLAM). SLAM is a computational problem of building or updating a map of an unknown environment while simultaneously tracking the positions of agents (e.g., robots, people) [62, 71]. Similar to IMU-based methods, recent studies have investigated the integration of machine learning techniques into the SLAM framework [4, 13, 32, 74, 83]. Although SLAM has been proven effective in numerous applications, its practical performance can still be influenced by factors such as the quality of the camera feed, lighting conditions, and the complexity and dynamics of the environment. A thorough site survey is also required to remove undesirable objects (like mirrors or texture-less walls) for reliable tracking via SLAM. In our study, we utilize SLAM techniques in a relatively controlled environment to provide a ground-truth trajectory, following previous work [21, 44, 70, 89, 90].

3 BACKGROUND

3.1 Motivating Scenarios

This paper studies indoor trajectory estimation for retail environments, which have become an attractive application domain for a variety of cutting-edge technologies [58]. Localization systems meet various demands in the retail industry, such as facilitating in-store navigation [54, 56] and inventory management [8]. Given trajectories of customers in a store, retailers can identify items that attracted interest but were not purchased, enabling targeted advertising [17, 45, 65].

Major retailers often operate multiple stores, expecting these systems to be easily deployable. However, the installation of extensive sensor networks and anchor devices, such as cameras, BLE beacons, or UWB anchors involve significant equipment and labor costs. Continuous site surveys for wireless localization in evolving environments can disrupt store operations. Furthermore, respecting customer privacy is crucial when tracking their in-store movements [15, 28, 34, 64, 88] to comply with laws and regulations such as the EU’s General Data Protection Regulation (GDPR). This is particularly important when location data are associated with personal information, such as purchase records. Data collection must be on an opt-in and out-out basis with explicit customer consent in advance. Despite their prevalence, security camera systems in retail settings do not inherently support these privacy safeguards, as they capture images of anyone regardless of consent.

Tab. 1 summarizes the key features of RETAILOPT against other available solutions. Our solution is driven by the growing popularity of smartphone applications for in-store location-based services [31, 48, 77, 85]. These retail apps provide location-specific advertisements, coupons, access to purchase records, store maps, and inventory data. The use of existing facilities will not incur additional maintenance costs as they must already be up-to-date as a vital

routine operation for retailers. Moreover, since IMU data is stored on the user’s smartphone by default, individuals have complete control over their own movement data. In practice, trajectory estimation may first take place on customer’s edge devices or in the cloud with limited access. Retailers can then obtain the trajectory data from customers only with explicit consent.

3.2 Preliminaries

This section provides the mathematical definition of our trajectory estimation task. We consider a bounded 2D environment $\Omega = [0, 1]^2$. The trajectory of a target person is defined over a discrete time interval $[1, T]$ and is represented by a sequence $P = (p_1, \dots, p_T)$, where $p_t \in \Omega$ is the position of the person at time t .

Localization Anchors and Spatial Cues from Retail Facility Information. Our key idea is to leverage the store map and purchase records for a target person to create *anchors*, referential landmarks with known global positions. As shown below, we consider three types of spatial cues.

- Time-unknown anchors: $\mathcal{X}_{\text{tu}} = \{(x_j, \phi)\}_{j=1}^J$, $x_j \in \Omega$, provide a small set of locations that the target person has certainly visited, although *it remains unknown when these visits happened*.³ For example, if an apple is listed in the target person’s receipt, it is highly probable that the person visited the shelf of apples in the fruit section, whose location is available in the store map. However, the order of items in the receipt does not necessarily reflect the chronological order of the person’s interactions with those items, leaving the exact timing of each visit unknown.
- Time-known anchors: $\mathcal{X}_{\text{tk}} = \{(x_k, t_k)\}_{k=1}^K$, $(x_k, t_k) \in \Omega \times \mathbb{N}$, present a pair of locations and timestamps when these locations are visited. Though less frequently than time-unknown anchors, time-known anchors are also available for practical retail scenarios, *e.g.*, when making payments at a POS register system or opening a smartphone app near the entrance to earn rewards.
- Obstacle layout: $\Omega_{\text{obs}} \subset \Omega$, indicates locations and sizes of physical obstacles such as walls or pillars in the environment, which can be easily extracted from the store map.

Relative Trajectory from Smartphone’s Motion Data. Furthermore, the target person’s smartphone provides continuous access to device acceleration, angular rate, and orientation data from its IMU. These data are utilized to estimate a relative motion trajectory of the target via inertial navigation, which we denote as $Q = (q_1, \dots, q_T)$, $q_t \in \mathbb{R}^2$. In line with prior work [21, 89], here we assume that the smartphone device is not necessarily attached rigidly to the person’s body but is held loosely in hand, in a pocket, or in a bag. Any inertial navigation algorithm would essentially work as long as it offers reasonable motion estimation accuracy. See Sec. 5.2 for the concrete algorithm used in our experiment.

Key Technical Challenge. Relative trajectories from smartphone’s IMU are obtained densely but can be erroneous and drifted due to inherent inertial noises. On the other hand, time-unknown and time-known anchors indicate actual global locations but can be available only sparsely for each journey (*e.g.*, less than ten for hundreds of meters of movement). This leads to our key challenge: *How can we integrate Q and $\mathcal{X}_{\text{tu}}, \mathcal{X}_{\text{tk}}, \Omega_{\text{obs}}$ to estimate P ?*

Baseline Approaches. The aforementioned problem is nontrivial to solve by simply applying existing methods. Since time-unknown anchors, \mathcal{X}_{tu} , do not contain timestamp information, it is not feasible to merely interpolate them to reconstruct the entire trajectory P . Point-set registration, briefly introduced in Sec. 2, could find a non-rigid

³Here, ϕ indicates that no time information is available for x_j , making the notation of \mathcal{X}_{tu} consistent with that of \mathcal{X}_{tk} .

transformation to match relative trajectory Q and global locations of anchors $\mathcal{X}_{\text{tu}}, \mathcal{X}_{\text{tk}}$. However, existing registration methods may exhibit limited performance due to the extremely unbalanced number of points between Q and $\mathcal{X}_{\text{tu}}, \mathcal{X}_{\text{tk}}$ as well as highly complicated nonlinear transformations between them while considering physical obstacles in Ω_{obs} .

4 PROPOSED SYSTEM

The proposed system, RETAILOPT, estimates a trajectory P for a target person from the relative motion trajectory Q , time-unknown anchors \mathcal{X}_{tu} , time-known anchors \mathcal{X}_{tk} , and the obstacle layout Ω_{obs} . As outlined in Fig. 2, RETAILOPT involves continuous and discrete optimization procedures. Initially, we transform Q to align more closely with actual locations indicated by \mathcal{X}_{tu} and \mathcal{X}_{tk} . We achieve this by optimizing a neural network, hereafter referred to as the *transformation network*, through gradient descent with back-propagation. Subsequently, we further refine the transformed trajectory by projecting it onto the valid space, *i.e.*, $\Omega \setminus \Omega_{\text{obs}}$, based on a Viterbi algorithm. This ensures that the final trajectory does not collide with obstacles.

4.1 Continuous Optimization with Transformation Network

Our transformation network accepts $Q, \mathcal{X}_{\text{tu}}, \mathcal{X}_{\text{tk}}$, and time indices $[1, \dots, T]$ as input to provide per-step displacements, $\Delta = (\delta_1, \dots, \delta_T)$, $\delta_t \in \mathbb{R}^2$, such that a transformed trajectory $Q' = (q'_1, \dots, q'_T)$, $q'_t = q_t + \delta_t$ passes through the locations in $\mathcal{X}_{\text{tu}}, \mathcal{X}_{\text{tk}}$. The use of highly expressive neural networks enables us to derive a complex non-linear transformation while considering the spatiotemporal continuity of Q as well as optimization targets indicated by $\mathcal{X}_{\text{tu}}, \mathcal{X}_{\text{tk}}$. Moreover, its optimization can be readily implemented on sophisticated deep learning frameworks with flexible automatic differentiation functionalities (*e.g.*, JAX [5]), allowing for efficient execution on GPUs.

Let us first define the objective function for optimizing the transformation network. The function measures the discrepancy between Q' and $\mathcal{X}_{\text{tu}}, \mathcal{X}_{\text{tk}}$ as follows:

$$L(Q', Q, \mathcal{X}_{\text{tu}}, \mathcal{X}_{\text{tk}}) = L_{\text{match}}(Q', \mathcal{X}_{\text{tu}}, \mathcal{X}_{\text{tk}}) + L_{\text{bound}}(Q') + \lambda L_{\text{reg}}(Q', Q), \quad (1)$$

where L_{match} is a matching term, L_{bound} is a boundary constraint, and L_{reg} is a regularizer with coefficient λ , each detailed below.

Matching Term. For each combination of a single anchor $(x, \cdot) \in \mathcal{X}_{\text{tu}} \cup \mathcal{X}_{\text{tk}}$ and transformed position q'_t at time t , we evaluate the squared distance, $(q'_t - x)^2$, as well as a matching confidence $w_{(q'_t, t, x)}$ quantifying how likely q'_t is to be actually located at x at time t . In the matching term, L_{match} , we take into account the matching that yields the highest value for the product of the discrepancy and confidence for each time t , defined as follows:

$$L_{\text{match}}(Q', \mathcal{X}_{\text{tu}}, \mathcal{X}_{\text{tk}}) = \sum_t \left(\max_{(x, \cdot) \in \mathcal{X}_{\text{tu}} \cup \mathcal{X}_{\text{tk}}} w_{(q'_t, t, x)} (q'_t - x)^2 \right). \quad (2)$$

If x is from time-known anchors, the matching confidence $w_{(q'_t, t, x)}$ is given as:

$$w_{(q'_t, t, x)} = \begin{cases} 1 & \text{if } (x, t') \in \mathcal{X}_{\text{tk}}, t' = t \\ 0 & \text{else if } (x, t') \in \mathcal{X}_{\text{tk}}, t' \neq t, \end{cases} \quad (3)$$

which produces the highest confidence if and only if t is in \mathcal{X}_{tk} . Evaluating $w_{(q'_t, t, x)}$ for time-unknown anchors is non-trivial because it is unknown at which time t we should match q'_t against x . To address such temporal uncertainty,

we propose the following ‘soft’-matching:

$$w(q'_t, t, x) = \frac{\exp(-(q'_t - x)^2 / \tau)}{\sum_t \exp(-(q'_t - x)^2 / \tau)}, \text{ if } (x, \cdot) \in \mathcal{X}_{\text{tu}}. \quad (4)$$

This is a soft-max operation on the negative of squared distance $(q'_t - x)^2$ with temperature τ , providing a higher confidence weight for pairs (q'_t, x) that are closer to each other at every optimization step.

Boundary Constraint and Regularizer. The boundary constraint, $L_{\text{bound}}(Q')$, ensures that the transformed position q'_t remains within the bounded 2D space $\Omega = [0, 1]^2$, defined as follows:

$$L_{\text{bound}}(Q') = \max_t (\text{ReLU}(-q'_t) + \text{ReLU}(q'_t - 1))^2, \quad (5)$$

where $\text{ReLU}(\cdot)$ is a rectified linear unit (ReLU) function that imposes a penalty for positions outside $[0, 1]^2$. Finally, we introduce a L1 regularizer for motion velocities:

$$L_{\text{reg}}(Q', Q) = \sum_t \left\| (q'_t - q'_{t-1}) - (q_t - q_{t-1}) \right\| = \sum_t \|\delta_t - \delta_{t-1}\|, \quad (6)$$

which prevents the motion velocity $q'_t - q'_{t-1}$ from changing too much from the original one $q_t - q_{t-1}$ in every step. This allows us to preserve the person’s walking speed initially estimated using inertial navigation.

Network Architecture. We design the architecture of the transformation network as follows:

$$\begin{aligned} H &= (h_1, \dots, h_T) = \text{attn}(Q^\top W_q, XW_k, XW_v), \\ z_t &= \text{cat}(q_t, h_t, t), \\ \delta_t &= \text{MLP}(z_t). \end{aligned} \quad (7)$$

$X \in \Omega^{J+K}$ is a stack of all locations contained in \mathcal{X}_{tu} and \mathcal{X}_{tk} . $\text{attn}(\cdot, \cdot, \cdot)$ is a scaled dot-product attention layer [78] with $W_q, W_k, W_v \in \mathbb{R}^{2 \times d}$ and $H \in \mathbb{R}^{T \times 2}$. $\text{cat}(\cdot, \cdot, \cdot)$ is a concatenation of vectors. MLP is a standard multi-layer perceptron with the ReLU activation for each layer except the last one. The use of the attention layer allows the network architecture to flexibly accommodate trajectories Q and anchors X of arbitrary lengths within the same framework.

Optimization Strategy. Importantly, all the terms in Eq. (1) as well as network layers in Eq. (7) are differentiable with respect to per-step displacements, $\delta_t = q'_t - q_t$. This makes it possible to adopt a standard gradient descent technique to minimize the objective with respect to δ_t , and consequently with respect to the parameters of the transformation network via back-propagation. Furthermore, the temperature parameter, τ in Eq. (4), can also be optimized simultaneously through gradient descent. Note that this continuous optimization procedure is *not* a standard deep learning task that learns a neural network from training data. We optimize the parameters of our neural network for every single problem instance of $(Q, \mathcal{X}_{\text{tu}}, \mathcal{X}_{\text{tk}})$ obtained from a single person’s trajectory. This allows our system to be deployed to new environments without additional training data collection.

4.2 Discrete Optimization for Obstacle Avoidance

Given a transformed trajectory Q' that is globally localized based on time-unknown and time-known anchors, our next step is to project Q' onto the valid space $\Omega \setminus \Omega_{\text{obs}}$ to avoid passing through obstacle regions in Ω_{obs} . We solve this problem through a discrete optimization base on a Viterbi algorithm, as summarized in Alg. 1.

Algorithm 1 Project Trajectory onto Valid Space via Viterbi Algorithm

Require: Input trajectory $Q' = (q'_1, \dots, q'_T) \in \Omega^T$; Environment Ω ; Obstacle layout Ω_{obs}

Ensure: Collision-free trajectory $\zeta \in (\Omega \setminus \Omega_{\text{obs}})^T$

- 1: $\mathcal{V} \leftarrow \{v \mid v \in \Omega \setminus \Omega_{\text{obs}}\} \cup \{v \mid v \in Q'\}$ ▷ Sample vertices from the valid space and concatenate them with Q' .
- 2: $\mathcal{E} \leftarrow \text{Validate}(\mathcal{V}, \Omega_{\text{obs}})$ ▷ Validate all pairs of vertices to span collision-free edges.
- 3: $D \leftarrow 0^{|\mathcal{V}|^2}$, $\mathcal{N} \leftarrow \{1, \dots, |\mathcal{V}|\}$ ▷ Initialize the edge cost matrix between vertices for pairwise terms.
- 4: **for** $i, j \in \mathcal{N}^2$ **do**
- 5: $D_{i,j} \leftarrow \begin{cases} \beta \cdot \|v_i - v_j\|_2 & (v_i, v_j) \in \mathcal{E} \\ \infty & \text{otherwise} \end{cases}$
- 6: **end for**
- 7: $M \leftarrow 0^{|\mathcal{V}| \times T}$, $J \leftarrow 0^{|\mathcal{V}| \times T}$ ▷ Instantiate the matrices for cost-so-far (M) and selected indices (J).
- 8: **for** $t = 1, \dots, T$ **do**
- 9: **for** $i \in \mathcal{N}$ **do**
- 10: **if** $t = 1$ **then**
- 11: $M_{i,t} \leftarrow \|v_i - q'_t\|_2$
- 12: $J_{i,t} \leftarrow \phi$
- 13: **else**
- 14: $M_{i,t} \leftarrow \min_{j \in \mathcal{N}} \{M_{j,t-1} + \|v_i - q'_t\|_2 + D_{i,j}\}$
- 15: $J_{i,t} \leftarrow \arg \min_{j \in \mathcal{N}} \{M_{j,t-1} + \|v_i - q'_t\|_2 + D_{i,j}\}$
- 16: **end if**
- 17: **end for**
- 18: **end for**
- 19: $\zeta = \text{Backtrack}(J)$ ▷ Backtrack selected indices in J to derive the final trajectory.

Specifically, we first construct a 2D undirected graph that approximates the solution space, where vertices $\mathcal{V} \subset \Omega$ are the concatenation of trajectory Q' and random positions sampled uniformly from the valid space $\Omega \setminus \Omega_{\text{obs}}$. For each pair of vertices $(v, v') \in \mathcal{V}^2$, we validate if the straight line segment between them does not collide with any obstacle region in Ω_{obs} , and span edges $\mathcal{E} \subset \mathcal{V}^2$ between valid vertex pairs ('Validate' in Alg. 1). Each edge is assigned a cost by the L2 distance between vertices, $\|v - v'\|_2$.

On the constructed graph, a trajectory can be represented by a sequence of connected vertices $\zeta = (v_1, \dots, v_T) \in \mathcal{V}^T$, $(v_{t-1}, v_t) \in \mathcal{E}$. We define a cost $c(\zeta, Q')$ for each trajectory as follows:

$$c(\zeta, Q') = \sum_{t=1}^T \|v_t - q'_t\|_2 + \beta \sum_{t=2}^T \|v_t - v_{t-1}\|_2, \quad (\beta) \quad (8)$$

where β is a hyperparameter. Intuitively, the first unary term ensures trajectories stay as close to the original one Q' as possible within the valid space, while the second pairwise term encourages them to be shorter. Viterbi algorithm (L8-L19 in Alg. 1) can efficiently find the lowest-cost trajectory on the given graph, which we refer to as the final output.

5 DATA COLLECTION

For quantitative evaluation, we collected new data of people navigating indoor environments. Our study received the approval from the ethics review board of the author's affiliation. The collected data will be published online as a new dataset for research purposes.

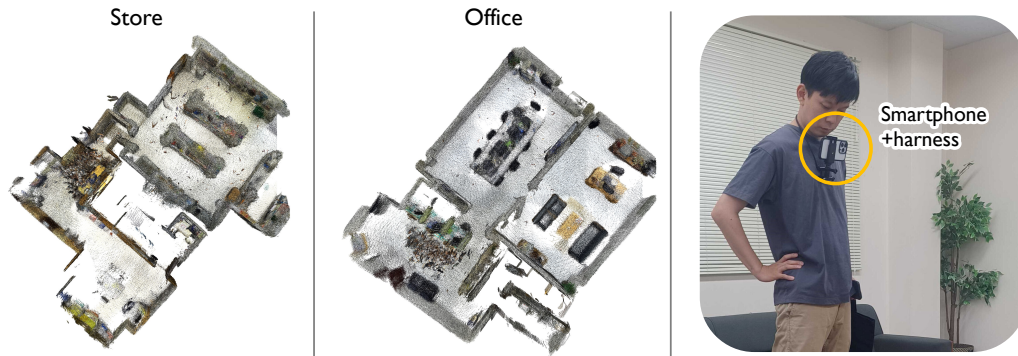


Fig. 3. **Data Collection Environments.** Left and center: Aerial point-of-view images of the environments, reconstructed from dense point clouds. Right: An example of a participant equipped with a smartphone around the neck.

5.1 Setup

Environments. As shown in Fig. 3, our data collection took place in two indoor environments: (a) *store*, a retail store consisting of a selling area with multiple shelves and a backyard, and (b) *office*, a travel agency office consisting of a hallway and two rooms with multiple desks. Both environments were approximately 100 m². We chose the store environment as our main application domain is retail, and the office environment to demonstrate the potential applicability of our system to other scenarios such as office maintenance and security patrol tasks.

Systems. We used two smartphones (iPhone 14 Pro) to record the participant’s motion in two distinct ways. One smartphone (smartphone A) was hung from the participant’s neck using a harness and loosely fixed to ensure the camera was always horizontal and facing forward (see Fig. 3 right). We performed visual-LiDAR SLAM [39] to obtain a ground-truth trajectory, as done in prior work [21, 89, 90], at a frequency of 5 Hz. The other smartphone (smartphone B) was either held in hand, placed in a pocket, or put in a bag, as per the experimenter’s instructions. We recorded 3-degree-of-freedom (DoF) accelerations, 3-DoF angular rates, and 3D orientations of both devices at 50 Hz⁴ using a smartphone app.⁵ The timestamps between SLAM trajectories and IMU data of the two smartphones were accurately synchronized based on the NTP server.

Data Collection Procedure. We recruited 15 participants (10 males and 5 females) from the author’s affiliation. All participants were familiar with operating a smartphone and had no difficulty walking at a normal speed. We asked participants to ‘mimic’ shopping activities while not accessing actual retail systems (*i.e.*, retail apps and POS cash registers) for two main reasons: 1) Participant’s behaviors should be sufficiently controlled for systematic evaluation; 2) Intervention in retail systems that are currently operational is not always feasible in practice during the fundamental research stage. Specifically, each participant, equipped with the smartphones, was asked to visit four specified locations in the environment. The order of visiting these locations was the same for all participants, but the specific routes between locations were left to the participant’s discretion. Upon arriving at each location, participants were instructed to pause for a few seconds to view a poster displayed there, simulating shopping behavior. The exact stationary position varied among participants, but remained within the range where the poster was visible (about 0.5-1 m). Participants

⁴While the iPhone’s IMU is capable of operating at a higher sampling frequency such as 100 Hz, our pilot study has verified that reducing the sampling rate to 50 Hz does not significantly impact the efficiency of the subsequent inertial navigation.

⁵<https://www.tszheichoi.com/sensorlogger>

Table 2. **Statistics of Our New Dataset.** We recorded the movements of 15 participants, more specifically, the IMU data from a pair of smartphones and the ground-truth trajectories estimated via visual-LiDAR SLAM [39], in two different indoor environments: a retail store and a travel agency office. The entire data collection procedure received approval from the ethics review board, allowing online publication of the data for research purposes.

Environment	# Valid sessions	Recorded time (total/min/max)	Travel distance (total/min/max)
Store	118	12.0 hours / 175 sec / 962 sec	15.5 km / 70 m / 389 m
Office	120	10.8 hours / 154 sec / 674 sec	15.2 km / 65 m / 463 m

were permitted to walk at any pace and pause whenever they wished, as long as their behavior mimicked typical indoor walking activity. After visiting all the locations, they were instructed to return to the starting point. This process was repeated three times, with the same set of four locations, while varying the way smartphone B was carried (*i.e.*, held in hand, placed in a pocket, or put in a bag), resulting in a single session of approximately three minutes. When holding smartphone B in their hands, participants either pretended to operate it or walked while swinging their arm with the phone in hand. The location and size of the pocket where smartphone B was placed varied among participants. Although all participants used the same bag, the manner in which the bag was carried was completely different from one participant to another. After a short break and device re-calibration, participants conducted the next session with a different set of four locations. Each participant completed three sessions for both the store and office environments. We also gathered additional data by asking participants to freely walk around the environments, while periodically altering how they held smartphone B. This data was used for training neural inertial navigation models introduced in the next section. In total, we collected about one hour of recording for each participant. Tab. 2 summarizes the statistics of collected data.

5.2 Data Processing

Coordinate Alignment. Device coordinate systems for IMU sensor data are different between smartphones A and B. Moreover, the coordinate systems regarding SLAM trajectories are different for each recording. To align such heterogeneous systems, we performed the following three-step calibration procedure. At the beginning of each recording, we keep the two smartphones stationary in the same direction for a few seconds. Their device orientations at that period are then used to find their relative 3D angle and rotate all the data from smartphone B with the angle to be aligned with those of smartphone A. Next, we further rotate accelerations and angular rates with the device orientations to be represented in the coordinate system consistent with that of SLAM trajectories, which is also referred to as heading-agnostic coordinate frames (HACF) [89]. Finally, we aggregate several collected SLAM data to construct a dense point cloud for each environment, with which we align all SLAM trajectories and corresponding IMU data in the same coordinate system.

Inertial Navigation. To generate relative motion trajectories Q , we re-implemented RoNIN [89], a data-driven inertial navigation method that uses a neural network to regress velocity vectors from IMU data. We split 15 participants into 10 training, 2 validation, and 3 test subsets. We chose the RoNIN-ResNet model consisting of four residual blocks (1D convolution layers followed by batch normalization and ReLU activation layers and skip connections) followed by three fully-connected layers each with ReLU activation except for the last one. It accepts 50-frame (*i.e.*, 1 second) sequences of concatenation of accelerations and angular rates as input to predict average velocity vectors for the same time period. The model was trained for each environment independently, to minimize the mean squared error loss

between predicted and ground-truth velocity vectors using the Adam optimizer [36]. The learning rate, batch size, and number of epochs were set to (0.0001, 64, 100). We saved the model checkpoints with the lowest validation loss, and swapped the checkpoints to use the model trained on the store environment data to estimate trajectories for the office, and vice versa. This ensured no overlaps between participant individuals and environments in the training and test subsets, representing a practical setup. For each sample in the test subsets, we applied the trained model to estimate the average velocity over 50 frames every 25 frames, yielding relative motion trajectories sampled at 2 Hz.

Simulating Retail Facility Information. We manually specified anchors to simplify the experiment protocol, while in practical retail setups they can be acquired from the store map and purchase records. Specifically, we split each session data into three sub-sequences based on how smartphone B was held (*i.e.*, pocket, hand, bag), and treated the first and last ground-truth locations with timestamps as time-known anchors, \mathcal{X}_{tk} . The four pre-determined locations were treated as time-unknown anchors, \mathcal{X}_{tu} . Moreover, the obstacle layout Ω_{obs} was created from the point cloud, although it can be identified from a store map in practice.

6 EXPERIMENT

We systematically evaluate the performance of the RETAILOPT system on five diverse environments: two from our new dataset presented in the previous section and the remaining three from a public dataset [21].

6.1 Evaluation Procedure

Implementation Details. RETAILOPT has several options for its architectural design and optimization strategy. λ, β in Eq. (1) and Eq. (8) were set to $\lambda = \beta = 0.01$. In the transformation network, MLP consists of two layers with the channel dimensions 64 and 128. For the attention layer (attn), feature dimension d of W_q, W_k, W_v were all set to $d = 32$. The temperature parameter, τ in Eq. (4), was initially set to $\tau = 100$ and then optimized through gradient descent. The optimization of the transformation network was done for 1000 iterations using the Adam optimizer [36] with a learning rate of 0.001. For the discrete optimization procedure, 1000 vertices were sampled from the uniform distribution to construct a graph.

Baseline Methods. The primary focus of this experiment is on the fusion of relative motion trajectories derived from IMU data, time-unknown/known anchors, and the obstacle layout for indoor trajectory estimation. This challenge has not been addressed in any prior work. For instance, adopting existing fusion approaches for IMU and wireless localization [22, 35, 41, 79, 93] is not feasible due to the lack of time information for most of our anchors. Instead, we have compared our approach with the following relevant methods, each utilizing variable sets of input data.

TSP Solver (w/ anchors and obstacle layout) This baseline solves a traveling salesman problem (TSP) to determine the shortest route that connects the two time-known anchors while visiting all the time-unknown anchors. Subsequently, we linearly interpolate the anchors to estimate a dense trajectory of length T with a constant velocity. Finally, we apply the same Viterbi-based discrete optimization procedure as RETAILOPT to project the trajectory onto the valid space.

RoNIN [89] (w/ IMU and time-known anchors) This is a popular machine-learning-based inertial navigation method that estimates relative motion trajectories from IMU data, which is also employed in our system to provide initial relative trajectories as in Sec. 5.2. We manually geo-localize the initial locations of the trajectories to the start locations provided as time-known anchors. Note that we refrained from applying the discrete

optimization procedure used in the proposed method as well as other baselines here, as doing so without alignments to anchors did not improve performances.

CPD Solver (w/ IMU, time-unknown/known anchors, and obstacle layout) This approach allows us to estimate nonrigid transformations between the relative trajectories from IMU and time-unknown/known anchors through coherent point drift (CPD) point-set registration. We evaluated three variants: nonrigid CPD [50], constrained CPD [18], and Bayesian CPD [23], which are all implemented in [33]. The constrained CPD uses time-known anchors as the constraints from known point-to-point correspondences. All these methods are followed by the same discrete optimization procedure using the obstacle layout as RETAILOPT, thus using exactly the same set of input data.

6.2 Results on Our New Dataset

Quantitative Results. We evaluated the positional error between the estimated and ground-truth trajectories, which is reported in meters and averaged over time steps at 2 Hz. We hypothesize that the performance of RETAILOPT would depend on the quality of the initial relative trajectories provided by RoNIN. As one of the sources for erroneous outputs from RoNIN is the variability of smartphone poses, we systematically calculated the positional errors separately for each phone’s handling style: neck (from smartphone A’s IMU), pocket, bag, and hand (from smartphone B). As shown in Tab. 3, RETAILOPT estimates participant’s trajectories more accurately than baseline methods. The performances of TSP and RoNIN were limited due to their access being restricted to only anchors and obstacle layouts (in the case of TSP) or dense motion trajectories (for RoNIN). Among the CPD family, nonrigid CPD proved to be the most robust, suggesting that point-to-point constraints and Bayesian inferences for the other CPD methods were not particularly effective in further enhancing the registration accuracy. For the RETAILOPT, the average positional error is less than 1.3 m particularly when the smartphone was hung from the neck or in a pocket. It was challenging for all the methods to accurately estimate trajectories when the smartphone was otherwise held by the hand or put in a bag, owing to the degraded accuracy of RoNIN that provided initial trajectories. We observe that the pose and motion of smartphones for these conditions were much more diverse and dynamic, making IMU data noisy and RoNIN’s estimation unreliable.

Qualitative Results. Fig. 4 visualizes some typical examples of results from TSP, RoNIN, nonrigid CPD, and RETAILOPT. RETAILOPT can estimate trajectories accurately even for challenging cases where the other baselines failed to work (the third example), but could provide inaccurate results if the RoNIN’s prediction is completely corrupted (the bottom example). Nonrigid CPD and TSP baselines could work on simple trajectories, but their performances significantly degraded for complex problems. We found that there were often significant spatial overlaps between RETAILOPT’s trajectories and ground-truth ones. This indicates that the main source of errors in RETAILOPT comes from temporal discrepancy rather than spatial one.

Ablation Study. To further analyze the performance of RETAILOPT, we conducted an ablation study. In Tab. 4, we compare the complete version of our method against its degraded variants: **w/o attn** that does not have the attention layer attn, *i.e.*, $z_t = \text{cat}(q_t, t)$; **w/o time** that instead omits time indices, *i.e.*, $z_t = \text{cat}(q_t, h_t)$, **# layers = 1** that uses a shallow MLP with a single hidden layer, and **w/o discrete opt** that omits the discrete optimization procedure. Although the performance differences are relatively small compared to the improvements from baseline methods, we can still confirm that the complete version performed the best or second best in many cases, showing that all the technical components contributed to the reliable trajectory estimation by RETAILOPT.

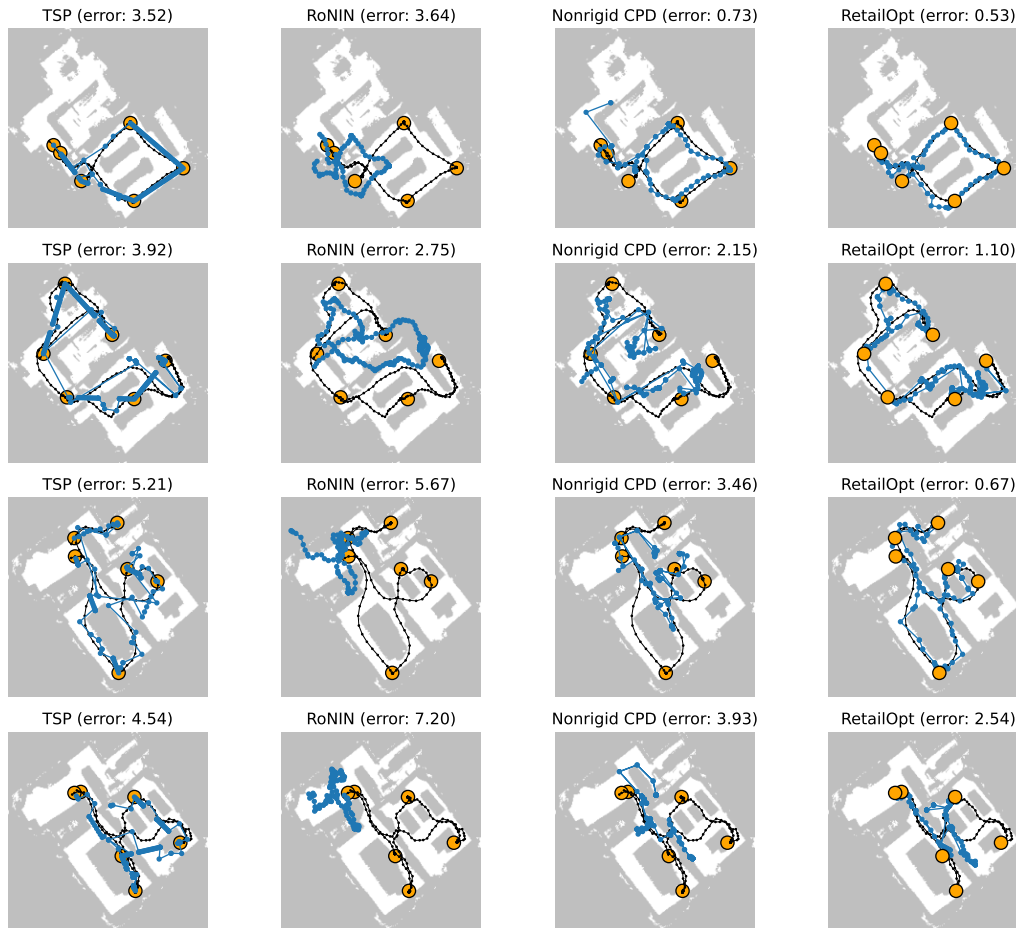


Fig. 4. **Qualitative Results on Our New Dataset.** The estimated and ground-truth trajectories are visualized with blue and black lines, respectively. Obstacle regions are colored in gray, and anchors are annotated with orange circles.

Computation Times. Fig. 5 shows computation times required to estimate a single trajectory sample by TSP, RoNIN, nonrigid CPD, and RETAILOPT, measured on either Intel(R) Xeon(R) Gold 6226 CPU @ 2.70GHz or NVIDIA Tesla T4. When executed on GPUs, RETAILOPT can process trajectories of length $T = 1280$ (corresponding to approximately 640 sec) with less than 2 seconds, which is much faster than the nonrigid CPD that performed the best among the baselines. This is because our overall pipeline can be built upon a well-established deep learning framework, more specifically JAX [5] in our implementation, to fully exploit GPU resources in both continuous and discrete optimization procedures. TSP and RoNIN can run much faster, but their trajectory estimation error are significantly worse as reported in Tab. 3.

6.3 Results on Inertial Localization Dataset

Data Preprocessing. In addition to our new dataset, we utilized the Inertial Localization Dataset [21], which includes over 50 hours of IMU data recorded in two outdoor environments (University A: $62.8 \times 84.4 \text{ m}^2$; University B: 57.6×147.2

Table 3. **Comparisons of Average Positional Error (m) on Our New Dataset.** The **best** and second-best methods for each condition are highlighted in bold and underlined, respectively.

	Store				Office			
	neck	pocket	hand	bag	neck	pocket	hand	bag
TSP	3.08	2.60	3.16	3.26	3.76	3.99	3.63	3.65
RoNIN [89]	3.09	3.27	4.23	4.74	3.50	4.48	5.09	6.41
Nonrigid CPD [50]	<u>2.11</u>	<u>1.51</u>	<u>2.90</u>	<u>3.29</u>	<u>1.47</u>	<u>2.26</u>	<u>2.46</u>	<u>3.36</u>
Constrained CPD [18]	4.11	3.74	4.58	5.42	3.83	3.55	3.38	5.12
Bayesian CPD [23]	3.17	2.26	3.48	3.38	2.18	2.71	3.09	3.58
RETAILOPT (Ours)	1.25	0.82	2.43	2.45	0.70	1.17	1.29	2.73

Table 4. **Ablation Study on Our New Dataset.** The **best** and second-best methods for each condition are highlighted in bold and underlined, respectively.

	Store				Office			
	neck	pocket	hand	bag	neck	pocket	hand	bag
Complete Version	1.25	0.82	2.43	2.45	<u>0.70</u>	1.17	1.29	<u>2.73</u>
w/o attn	<u>1.28</u>	<u>0.85</u>	2.58	<u>2.69</u>	0.66	0.98	1.32	2.78
w/o time	1.69	1.23	2.88	3.68	1.28	2.38	1.84	3.33
# layers = 1	1.29	1.02	2.46	3.51	0.80	1.41	1.66	3.39
w/o discrete opt	<u>1.28</u>	<u>0.85</u>	<u>2.45</u>	2.45	0.74	<u>1.16</u>	<u>1.31</u>	2.72

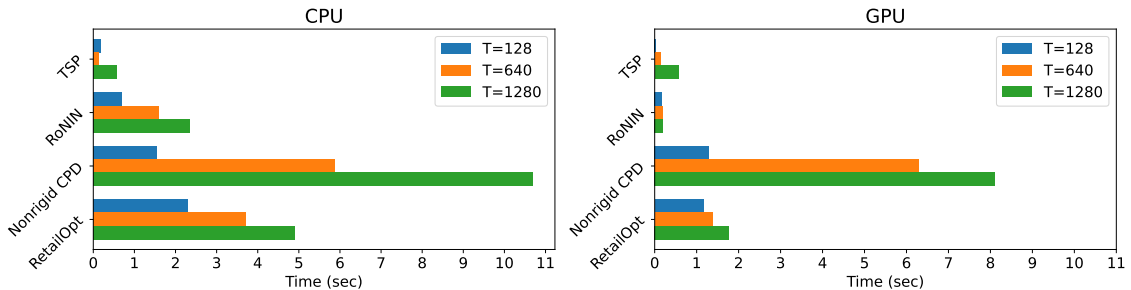
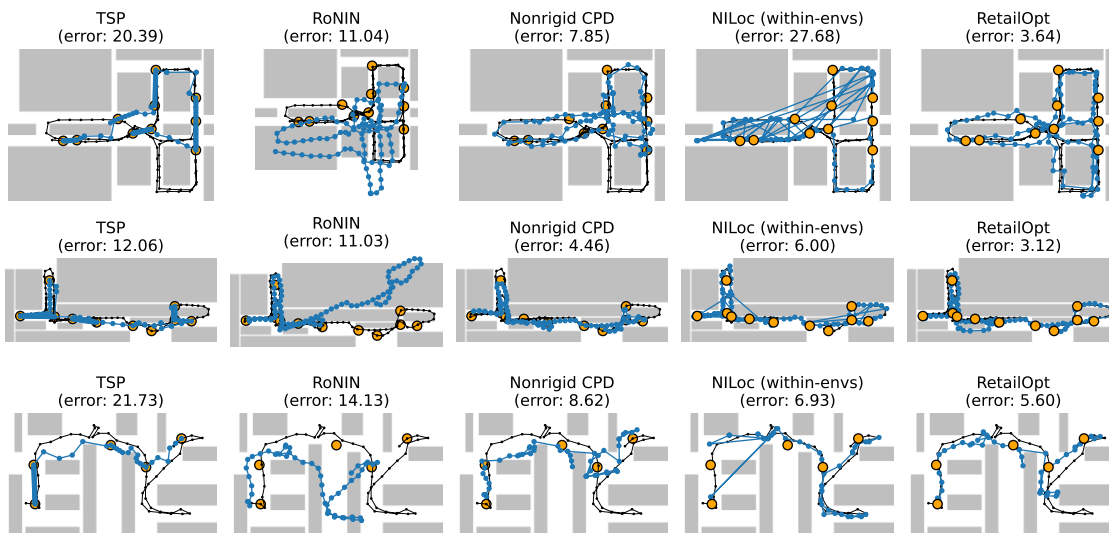


Fig. 5. **Computation Time Analysis.** We measured running times for selected methods to process a single test sample, with CPU: Intel(R) Xeon(R) Gold 6226 CPU @ 2.70GHz and GPU: NVIDIA Tesla T4.

m²) and one indoor environment (Office: 38.4 × 11.2 m²). Participants were instructed to navigate the environment while handling a pair of smartphones. One smartphone was held straight in one hand to record ground-truth trajectories via SLAM. The other smartphone was used freely, such as being held in the hand, used for a phone call, or stored in a pocket, although specific ways to hold it were not annotated. IMU data from both smartphones and SLAM data are all synchronized in time. As this dataset was originally created for general inertial localization purposes, it does not contain the information of obstacle layouts nor anchors. To make the dataset compatible with our problem setup, we performed the following manual pre-processing:

Table 5. **Comparisons of Average Positional Error (m) on Inertial Localization Dataset [21].** The **best** and second-best methods for each condition are highlighted in bold and underlined, respectively.

Distance traveled (m)	University A			University B			Office		
	100	200	400	100	200	400	100	200	400
TSP	12.95	17.46	22.55	11.88	20.86	20.54	5.65	6.69	10.53
RoNIN [89]	7.18	7.42	<u>8.19</u>	5.90	8.35	20.91	2.70	3.74	6.51
Nonrigid CPD [50]	<u>5.94</u>	7.37	8.39	2.79	12.81	14.61	4.45	4.74	5.06
Constrained CPD [18]	4.35	<u>5.45</u>	8.85	<u>1.94</u>	11.94	11.91	3.01	3.98	5.78
Bayesian CPD [23]	7.59	10.95	12.07	4.67	16.30	17.92	5.60	5.88	5.74
NILoc [21] (within-envs)	21.04	20.67	20.07	5.61	<u>4.65</u>	6.19	<u>2.62</u>	1.94	2.06
NILoc [21] (cross-envs)	45.25	41.82	42.16	53.60	55.77	52.76	16.56	14.71	13.56
RETAILOPT (Ours)	1.35	1.92	2.62	1.65	4.33	<u>8.93</u>	1.45	<u>2.16</u>	<u>3.38</u>


 Fig. 6. **Qualitative Results on Inertial Localization Dataset.** The estimated and ground-truth trajectories are visualized with blue and black lines, respectively. Obstacle regions are colored in gray, and anchors are annotated with orange circles.

Obstacle layout. For each environment, we aggregated all the ground-truth trajectories to identify the valid space (*i.e.*, walkable area) following the instructions of [21]. We then manually annotated multiple rectangles encompassing all obstacle regions to serve the obstacle layout Ω_{obs} .

Anchors. Additionally, we created some candidates for anchors by initially thinning the valid space and performing corner detection. As shown in Fig. 6, detected corners are located around the intersections or middle of the corridors that are close to the obstacles. For each data sample, we selected a part of the anchors that were within a pre-defined range (approximately 1 m) around the ground-truth trajectory, and used them as time-unknown anchors, \mathcal{X}_{tu} . We also used the starting and ending points of each trajectory as time-known anchors, \mathcal{X}_{tk} , similar to our new dataset.

Results. Tab. 5 presents the quantitative comparisons between RETAILOPT and the baselines. Given the longer ground-truth trajectories in larger environments and due to the lack of annotations for how smartphones were held, we instead reported average positional errors for several thresholds of distances being traveled. RETAILOPT consistently outperformed the other baselines. Although its performance depends on the accuracy of the original RoNIN’s trajectories and leads to increased errors with distance traveled, RETAILOPT was still able to estimate trajectories with less than approximately 4 m errors for University A and Office, and 9 m errors for University B, even for travels of 400 meters.

Comparisons with State-of-the-art Neural Inertial Localization. In addition to the baseline methods used in our user study, we evaluated NILoc [21], a state-of-the-art inertial localization method released with the dataset. The **NILoc (within-envs)** model was trained on the same environment, while the **NILoc (cross-envs)** model was trained on another environment. Comparing these two variants, we found that NILoc performed effectively only for the within-envs condition, demonstrating the necessity of a site survey for a large-scale data collection at each environment unlike the proposed system. Fig. 6 shows some qualitative examples.

Failure Cases. Fig. 6 bottom illustrates a typical failure case of RETAILOPT. Since RETAILOPT relies on anchors to globally align RoNIN’s trajectories, its performance inevitably deteriorates in regions where there are few anchors, such as the bottom-right of the environment. However, this is a common failure, also observed in other baselines that utilize anchor information, such as TSP and CPD methods. NILoc (within-envs) appears to be more accurate even in such regions, but it heavily relies on collecting training data from each target environment to build an environment-specific model, which is not always possible in practice.

7 DISCUSSIONS

Applications to New Environments. Our system does not require additional training data to be deployed in new environments. The accuracy of relative trajectories provided by inertial navigation is affected solely by the variability of how people walk and hold their smartphones, not by that of environments. Even if the trajectories are inaccurate in new environments, our system can refine them to be accurate, as empirically demonstrated in the experiments. This is a unique feature not available in NILoc [21] and other existing indoor positioning methods based on machine learning [52].

Integration with Other Sensors. Although RETAILOPT relies only on smartphone’s IMU and retailer-maintained facility information, it is easy to incorporate additional sensor data when provided. For example, passive sensing using dedicated tags installed in the environment could detect a person’s approaching or contact as timed events with anchors [8, 11, 19, 41, 47, 79]. Although our study focuses mainly on indoor localization, our system can be applied to outdoor environments where standard GPS could help improve the overall localization accuracy [35, 93].

When Smartphones are not Available. The use of smartphone apps is rapidly spreading in today’s retail scene [48, 77, 85]. We believe that active users will grant permissions for localizing themselves to get personalized information, just as they would do for other means of customer tracking. Nevertheless, continuous operation of IMUs, although they are energy efficient, would inevitably consume some battery power. When smartphones are not available, a possible alternative solution is to install IMUs on smart shopping carts consisting of a monitor and various sensing modules [9, 38, 40, 54, 67].

Limitations. Our system is currently built upon several assumptions, which could limit its potential use-cases. First, we presume a one-to-one match between items and their actual locations in environments, and people certainly visited those locations to interact with the items. If identical items are stored on multiple shelves, or if customers obtained those items without visiting the locations (*e.g.*, by asking companions to bring them the items,) this could obscure the locational cues from time-unknown anchors. Second, our approach assumes the store map and purchase records are provided by a single store. Estimating trajectories across multiple stores next to each other requires a unified data analysis platform that can access information from every store, certainly with different owners. While this is technically feasible, it implies the use of one retailer’s store information to improve the quality of trajectory data provided to another retailer, necessitating an appropriate incentive design and data protection framework. Finally, our system works only when customers purchase some items, and cannot reveal where the non-shoppers stopped. Nevertheless, we believe this constraint to be realistic, yet beneficial for knowing how much customers stopped at the shelves of the items they purchased and what other products they were interested in.

Applications to Other Domains. While the retail is a large application domain for our daily life, our system can also be applied to other scenarios, such as office maintenance and museum visits [37]. Many facilities have and can provide detailed map data, and it is now becoming common for people to install smartphone apps to record what items they have interacted with or which events they have experienced (*e.g.*, a list of locations to be inspected for office maintenance tasks, or that of artworks experienced in the museum). These data are analogous to the store map and purchase records for the retail scenario.

8 CONCLUSION

We have introduced RETAILOPT, a survey-free indoor trajectory estimation system specifically designed for retail environments. The proposed system exploits built-in retail facilities, namely the store map and purchase records, to extract locational anchors about where the target customer has or has not visited. These cues can be used to localize a relative motion trajectory, estimated from smartphone’s motion data via inertial navigation, in-store through continuous and discrete optimization procedures. The effectiveness of our system was confirmed through systematic experiments utilizing our new data collected from retail environments and a public inertial localization dataset.

Acknowledgements

This work was supported by JSPS KAKENHI Grant Number 23K24831.

REFERENCES

- [1] Apurva Bedagkar-Gala and Shishir K Shah. 2014. A survey of approaches and trends in person re-identification. *Image and Vision Computing* 32, 4 (2014), 270–286.
- [2] Asma Belhadi, Youcef Djenouri, Jerry Chun-Wei Lin, and Alberto Cano. 2020. Trajectory outlier detection: Algorithms, taxonomies, evaluation, and open challenges. *ACM Transactions on Management Information Systems (TMIS)* 11, 3 (2020), 1–29.
- [3] Paul J Besl and Neil D McKay. 1992. Method for registration of 3-D shapes. In *Sensor Fusion IV: Control Paradigms and Data Structures*, Vol. 1611. Spie, 586–606.
- [4] Michael Bloesch, Jan Czarnowski, Ronald Clark, Stefan Leutenegger, and Andrew J Davison. 2018. Codeslam—learning a compact, optimisable representation for dense visual slam. In *Proceedings of the IEEE Conference on Computer Vision and Pattern Recognition (CVPR)*. IEEE, 2560–2568.
- [5] James Bradbury, Roy Frostig, Peter Hawkins, Matthew James Johnson, Chris Leary, Dougal Maclaurin, George Necula, Adam Paszke, Jake VanderPlas, Skye Wanderman-Milne, and Qiao Zhang. 2018. *JAX: composable transformations of Python+NumPy programs*. <http://github.com/google/jax>
- [6] Antonio Brunetti, Domenico Buongiorno, Gianpaolo Francesco Trotta, and Vitoantonio Bevilacqua. 2018. Computer vision and deep learning techniques for pedestrian detection and tracking: A survey. *Neurocomputing* 300 (2018), 17–33.

- [7] Xiya Cao, Caifa Zhou, Dandan Zeng, and Yongliang Wang. 2022. RIO: Rotation-equivariance supervised learning of robust inertial odometry. In *Proceedings of the IEEE Conference on Computer Vision and Pattern Recognition (CVPR)*. IEEE, 6614–6623.
- [8] Anna Carreras, Marc Morenza-Cinos, Rafael Pous, Joan Melià-Seguí, Kamruddin Nur, Joan Oliver, and Ramir De Porrata-Doria. 2013. STORE VIEW: pervasive RFID & indoor navigation based retail inventory management. In *Proceedings of the ACM conference on Pervasive and Ubiquitous Computing Adjunct Publication (UbiComp Adjunct)*. 1037–1042.
- [9] P Chandrasekar and T Sangeetha. 2014. Smart shopping cart with automatic billing system through RFID and ZigBee. In *International Conference on Information Communication and Embedded Systems (ICICES2014)*. IEEE, 1–4.
- [10] Changhao Chen, Yishu Miao, Chris Xiaoxuan Lu, Linhai Xie, Phil Blunson, Andrew Markham, and Niki Trigoni. 2019. Motiontransformer: Transferring neural inertial tracking between domains. In *Proceedings of the AAAI Conference on Artificial Intelligence (AAAI)*, Vol. 33. 8009–8016.
- [11] Alseny Diallo, Zaixin Lu, and Xinghui Zhao. 2019. Wireless indoor localization using passive RFID tags. *Procedia Computer Science* 155 (2019), 210–217.
- [12] Yi Ding, Dongzhe Jiang, Yunhui Liu, Desheng Zhang, and Tian He. 2022. SmartLOC: Indoor Localization with Smartphone Anchors for On-Demand Delivery. *Proceedings of the ACM on Interactive, Mobile, Wearable and Ubiquitous Technologies (IMWUT)* 5, 4 (2022).
- [13] Chao Duan, Steffen Junginger, Jiahao Huang, Kairong Jin, and Kerstin Thurow. 2019. Deep learning for visual SLAM in transportation robotics: A review. *Transportation Safety and Environment* 1, 3 (2019), 177–184.
- [14] Ramsey Faragher and Robert Harle. 2015. Location fingerprinting with bluetooth low energy beacons. *IEEE Journal on Selected Areas in Communications* 33, 11 (2015), 2418–2428.
- [15] Kassem Fawaz, Kyu-Han Kim, and Kang G Shin. 2016. Privacy vs. reward in indoor location-based services. *Proceedings on Privacy Enhancing Technologies* (2016).
- [16] Ujwala Gawande, Kamal Hajari, and Yogesh Golhar. 2020. Pedestrian detection and tracking in video surveillance system: issues, comprehensive review, and challenges. *Recent Trends in Computational Intelligence* (2020), 1–24.
- [17] Anindya Ghose, Beibei Li, and Siyuan Liu. 2019. Mobile targeting using customer trajectory patterns. *Management Science* 65, 11 (2019), 5027–5049.
- [18] Vladislav Golyanik, Bertram Taetz, Gerd Reis, and Didier Stricker. 2016. Extended coherent point drift algorithm with correspondence priors and optimal subsampling. In *Proceedings of the IEEE Winter Conference on Applications of Computer Vision (WACV)*. IEEE, 1–9.
- [19] Jeremy Gummeson, James Mccann, Chouchang Yang, Damith Ranasinghe, Scott Hudson, and Alanson Sample. 2017. RFID light bulb: Enabling ubiquitous deployment of interactive RFID systems. *Proceedings of the ACM on Interactive, Mobile, Wearable and Ubiquitous Technologies (IMWUT)* 1, 2 (2017), 1–16.
- [20] Mahdi Hashemi and Hassan A Karimi. 2014. A critical review of real-time map-matching algorithms: Current issues and future directions. *Computers, Environment and Urban Systems* 48 (2014), 153–165.
- [21] Sachini Herath, David Caruso, Chen Liu, Yufan Chen, and Yasutaka Furukawa. 2022. Neural inertial localization. In *Proceedings of the IEEE Conference on Computer Vision and Pattern Recognition (CVPR)*. IEEE.
- [22] Sachini Herath, Saghar Irandoust, Bowen Chen, Yiming Qian, Pyojin Kim, and Yasutaka Furukawa. 2021. Fusion-dhl: Wifi, imu, and floorplan fusion for dense history of locations in indoor environments. In *Proceedings of the IEEE International Conference on Robotics and Automation (ICRA)*. IEEE, 5677–5683.
- [23] Osamu Hirose. 2020. A Bayesian formulation of coherent point drift. *IEEE Transactions on Pattern Analysis and Machine Intelligence (TPAMI)* 43, 7 (2020), 2269–2286.
- [24] Ville Honkavirta, Tommi Perala, Simo Ali-Loytty, and Robert Piché. 2009. A comparative survey of WLAN location fingerprinting methods. In *Proceedings of the IEEE Workshop on Positioning, Navigation and Communication*. IEEE, 243–251.
- [25] Xinyu Hou and Jeroen Bergmann. 2020. Pedestrian dead reckoning with wearable sensors: A systematic review. *IEEE Sensors Journal* 21, 1 (2020), 143–152.
- [26] Weiming Hu, Tieniu Tan, Liang Wang, and Steve Maybank. 2004. A survey on visual surveillance of object motion and behaviors. *IEEE Transactions on Systems, Man, and Cybernetics, Part C* 34, 3 (2004), 334–352.
- [27] Zhenfeng Huang, Shaojie Qiao, Nan Han, Chang-an Yuan, Xuejiang Song, and Yueqiang Xiao. 2021. Survey on vehicle map matching techniques. *CAAI Transactions on Intelligence Technology* 6, 1 (2021), 55–71.
- [28] Ari Juels, Ronald L Rivest, and Michael Szydlo. 2003. The blocker tag: Selective blocking of RFID tags for consumer privacy. In *Proceedings of the ACM conference on Computer and Communications Security (CCS)*. 103–111.
- [29] Kamol Kaemarungsi and Prashant Krishnamurthy. 2004. Modeling of indoor positioning systems based on location fingerprinting. In *Proceedings of the IEEE International Conference on Computer Communications (INFOCOM)*, Vol. 2. IEEE, 1012–1022.
- [30] Koji Kamei, Tetsushi Ikeda, Hiroyuki Kidokoro, Masayuki Shiomi, Akira Utsumi, Kazuhiko Shinozawa, Takahiro Miyashita, and Norihiro Hagita. 2011. Effectiveness of cooperative customer navigation from robots around a retail shop. In *Proceedings of the IEEE International Conference on Privacy, Security, Risk and Trust and International Conference on Social Computing*. IEEE, 235–241.
- [31] Ju-Young M Kang, Jung Mee Mun, and Kim KP Johnson. 2015. In-store mobile usage: Downloading and usage intention toward mobile location-based retail apps. *Computers in Human Behavior* 46 (2015), 210–217.
- [32] Peter Karkus, Shaojun Cai, and David Hsu. 2021. Differentiable slam-net: Learning particle slam for visual navigation. In *Proceedings of the IEEE Conference on Computer Vision and Pattern Recognition (CVPR)*. IEEE, 2815–2825.
- [33] Kenta-Tanaka et al. 2019. *probreg*. <https://probreg.readthedocs.io/en/latest/>

- [34] Eunhye Kim. 2021. In-store shopping with location-based retail apps: perceived value, consumer response, and the moderating effect of flow. *Information Technology and Management* 22, 2 (2021), 83–97.
- [35] Kwan-Soo Kim and Yoan Shin. 2021. Deep Learning-Based PDR Scheme That Fuses Smartphone Sensors and GPS Location Changes. *IEEE Access* 9 (2021), 158616–158631.
- [36] Diederik P Kingma and Jimmy Ba. 2015. Adam: A method for stochastic optimization. In *Proceedings of the International Conference on Learning and Representation (ICLR)*.
- [37] Alexandros Kontarinis, Claudia Marinica, Dan Vodislav, Karine Zeitouni, Anne Krebs, and Dimitris Kotzinos. 2017. Towards a Better Understanding of Museum Visitors’ Behavior through Indoor Trajectory Analysis. In *Proceedings of the International Conference on Digital Presentation and Preservation of Cultural and Scientific Heritage (DiPP)*, Vol. 7. 19–30.
- [38] Panos Kourouthanassis and George Roussos. 2003. Developing consumer-friendly pervasive retail systems. *IEEE Pervasive Computing* 2, 02 (2003), 32–39.
- [39] Mathieu Labbé and François Michaud. 2019. RTAB-Map as an open-source lidar and visual simultaneous localization and mapping library for large-scale and long-term online operation. *Journal of Field Robotics* 36, 2 (2019), 416–446.
- [40] Ruinian Li, Tianyi Song, Nicholas Capurso, Jiguo Yu, Jason Couture, and Xiuzhen Cheng. 2017. IoT applications on secure smart shopping system. *IEEE Internet of Things Journal* 4, 6 (2017), 1945–1954.
- [41] Xin Li, Jian Wang, and Chunyan Liu. 2015. A Bluetooth/PDR integration algorithm for an indoor positioning system. *Sensors* 15, 10 (2015), 24862–24885.
- [42] Yuqi Li, Zhe He, John Nielsen, and Gérard Lachapelle. 2015. Using Wi-Fi/magnetometers for indoor location and personal navigation. In *Proceedings of the International Conference on Indoor Positioning and Indoor Navigation (IPIN)*. IEEE, 1–7.
- [43] Jason Zhi Liang, Nicholas Corso, Eric Turner, and Avidesh Zakhor. 2013. Image based localization in indoor environments. In *Proceedings of the IEEE International Conference on Computing for Geospatial Research and Application*. IEEE, 70–75.
- [44] Wenxin Liu, David Caruso, Eddy Ilg, Jing Dong, Anastasios I Mourikis, Kostas Daniilidis, Vijay Kumar, and Jakob Engel. 2020. Tlio: Tight learned inertial odometry. *IEEE Robotics and Automation Letters (RA-L)* 5, 4 (2020), 5653–5660.
- [45] Xiaochen Liu, Yurong Jiang, Puneet Jain, and Kyu-Han Kim. 2018. TAR: Enabling fine-grained targeted advertising in retail stores. In *Proceedings of the ACM Annual International Conference on Mobile Systems, Applications, and Services (MobiSys)*. Association for Computing Machinery, 323–336.
- [46] Yin Lou, Chengyang Zhang, Yu Zheng, Xing Xie, Wei Wang, and Yan Huang. 2009. Map-matching for low-sampling-rate GPS trajectories. In *Proceedings of the ACM SIGSPATIAL International Conference on Advances in Geographic Information Systems*. ACM New York, NY, USA, 352–361.
- [47] Ahmed Mahmoud, Pedro Coser, Hamza Sadruddin, and Mohamed Atia. 2022. Ultra-wideband Automatic Anchor’s Localization for Indoor Path Tracking. In *Proceedings of the IEEE Sensors*. IEEE, 1–4.
- [48] Sebastian Molinillo, Rocío Aguilar-Illescas, Rafael Anaya-Sanchez, and Elena Carvajal-Trujillo. 2022. The customer retail app experience: Implications for customer loyalty. *Journal of Retailing and Consumer Services* 65 (2022), 102842.
- [49] Romero Morais, Vuong Le, Truyen Tran, Budhaditya Saha, Moussa Mansour, and Svetha Venkatesh. 2019. Learning regularity in skeleton trajectories for anomaly detection in videos. In *Proceedings of the IEEE Conference on Computer Vision and Pattern Recognition (CVPR)*. IEEE, 11996–12004.
- [50] Andriy Myronenko and Xubo Song. 2010. Point set registration: Coherent point drift. *IEEE Transactions on Pattern Analysis and Machine Intelligence (TPAMI)* 32, 12 (2010), 2262–2275.
- [51] Tayyab Naseer, Wolfram Burgard, and Cyrill Stachniss. 2018. Robust visual localization across seasons. *IEEE Transactions on Robotics* 34, 2 (2018), 289–302.
- [52] Ahasanun Nessa, Bhagawat Adhikari, Fatima Hussain, and Xavier N Fernando. 2020. A survey of machine learning for indoor positioning. *IEEE Access* 8 (2020), 214945–214965.
- [53] Eshed Ohn-Bar, João Guerreiro, Kris Kitani, and Chieko Asakawa. 2018. Variability in Reactions to Instructional Guidance during Smartphone-Based Assisted Navigation of Blind Users. *Proceedings of the ACM on Interactive, Mobile, Wearable and Ubiquitous Technologies (IMWUT)* 2, 3, Article 131 (2018), 25 pages.
- [54] Marina Paolanti, Daniele Liciotti, Rocco Pietrini, Adriano Mancini, and Emanuele Frontoni. 2018. Modelling and forecasting customer navigation in intelligent retail environments. *Journal of Intelligent & Robotic Systems* 91 (2018), 165–180.
- [55] Nathan Piasco, Désiré Sidibé, Cédric Demonceaux, and Valérie Gouet-Brunet. 2018. A survey on visual-based localization: On the benefit of heterogeneous data. *Pattern Recognition* 74 (2018), 90–109.
- [56] Aavek Purohit, Zheng Sun, Shijia Pan, and Pei Zhang. 2013. SugarTrail: Indoor navigation in retail environments without surveys and maps. In *Proceedings of the IEEE International Conference on Sensing, Communications and Networking (SECON)*. IEEE, 300–308.
- [57] Mohammed A Quddus, Washington Y Ochieng, and Robert B Noland. 2007. Current map-matching algorithms for transport applications: State-of-the-art and future research directions. *Transportation Research Part c: Emerging Technologies* 15, 5 (2007), 312–328.
- [58] Myriam Quinones, Ana M Díaz-Martín, and Mónica Gómez-Suárez. 2023. Retail technologies that enhance the customer experience: a practitioner-centred approach. *Humanities and Social Sciences Communications* 10, 1 (2023), 1–8.
- [59] Matteo Ridolfi, Abdil Kaya, Rafael Berkvens, Maarten Weyn, Wout Joseph, and Eli De Poorter. 2021. Self-calibration and collaborative localization for UWB positioning systems: A survey and future research directions. *ACM Computing Surveys (CSUR)* 54, 4 (2021), 1–27.
- [60] Royston Rodrigues, Neha Bhargava, Rajbabu Velmurugan, and Subhasis Chaudhuri. 2020. Multi-timescale trajectory prediction for abnormal human activity detection. In *Proceedings of the IEEE Winter Conference on Applications of Computer Vision (WACV)*. IEEE, 2626–2634.

- [61] Swapnil Sayan Saha, Sandeep Singh Sandha, Luis Antonio Garcia, and Mani Srivastava. 2022. TinyOdom: Hardware-aware efficient neural inertial navigation. *Proceedings of the ACM on Interactive, Mobile, Wearable and Ubiquitous Technologies (IMWUT)* 6, 2, Article 71 (2022).
- [62] Muhamad Risqi U Saputra, Andrew Markham, and Niki Trigoni. 2018. Visual SLAM and structure from motion in dynamic environments: A survey. *ACM Computing Surveys (CSUR)* 51, 2 (2018), 1–36.
- [63] Torsten Sattler, Bastian Leibe, and Leif Kobbelt. 2011. Fast image-based localization using direct 2d-to-3d matching. In *Proceeding of the International Conference on Computer Vision (ICCV)*. IEEE, 667–674.
- [64] Rabea Schrage, Lasse Meißner, Reinhard Schuette, and Peter Kenning. 2022. Acceptance of in-store apps: Factors that influence the intention to adopt location-based retail apps—Insights from Germany. *International Journal of Retail & Distribution Management* 50, 6 (2022), 760–777.
- [65] Stephanie Schwipfer, Severine Peche, and Gertrud Schmitz. 2020. Mobile Location-Based Services’ Value-in-Use in Inner Cities: Do a Customer’s Shopping Patterns, Prior User Experience, and Sales Promotions Matter? *Schmalenbach Business Review* 72, 4 (2020), 511–564.
- [66] Aleksandr Segal, Dirk Haehnel, and Sebastian Thrun. 2009. Generalized-icp. In *Robotics: Science and Systems*, Vol. 2. Seattle, WA, 435.
- [67] Mobeen Shahroz, Muhammad Faheem Mushtaq, Maqsood Ahmad, Saleem Ullah, Arif Mehmood, and Gyu Sang Choi. 2020. IoT-based smart shopping cart using radio frequency identification. *IEEE Access* 8 (2020), 68426–68438.
- [68] Héber Sobreira, Carlos M Costa, Ivo Sousa, Luis Rocha, José Lima, PCMA Farias, Paulo Costa, and A Paulo Moreira. 2019. Map-matching algorithms for robot self-localization: a comparison between perfect match, iterative closest point and normal distributions transform. *Journal of Intelligent & Robotic Systems* 93 (2019), 533–546.
- [69] Masato Sugasaki and Masamichi Shimosaka. 2017. Robust indoor localization across smartphone models with ellipsoid features from multiple rssi. *Proceedings of the ACM on Interactive, Mobile, Wearable and Ubiquitous Technologies (IMWUT)* 1, 3 (2017), 1–16.
- [70] Scott Sun, Dennis Melamed, and Kris Kitani. 2021. Idol: Inertial deep orientation-estimation and localization. In *Proceedings of the AAAI Conference on Artificial Intelligence (AAAI)*. AAAI Press.
- [71] Takafumi Taketomi, Hideaki Uchiyama, and Sei Ikeda. 2017. Visual SLAM algorithms: A survey from 2010 to 2016. *IPSP Transactions on Computer Vision and Applications (CVA)* 9, 1 (2017), 1–11.
- [72] Gary KL Tam, Zhi-Quan Cheng, Yu-Kun Lai, Frank C Langbein, Yonghuai Liu, David Marshall, Ralph R Martin, Xian-Fang Sun, and Paul L Rosin. 2012. Registration of 3D point clouds and meshes: A survey from rigid to nonrigid. *IEEE Transactions on Visualization and Computer Graphics* 19, 7 (2012), 1199–1217.
- [73] Stephen P Tarzia, Peter A Dinda, Robert P Dick, and Gokhan Memik. 2011. Indoor localization without infrastructure using the acoustic background spectrum. In *Proceedings of the International Conference on Mobile Systems, Applications, and Services (MobiSys)*. 155–168.
- [74] Zachary Teed and Jia Deng. 2021. Droid-slam: Deep visual slam for monocular, stereo, and rgb-d cameras. *Proceedings of the Annual Conference on Neural Information Processing Systems (NeurIPS)* 34 (2021), 16558–16569.
- [75] Carl Toft, Will Maddern, Akihiko Torii, Lars Hammarstrand, Erik Stenborg, Daniel Safari, Masatoshi Okutomi, Marc Pollefeys, Josef Sivic, Tomas Pajdla, et al. 2020. Long-term visual localization revisited. *IEEE Transactions on Pattern Analysis and Machine Intelligence (TPAMI)* 44, 4 (2020), 2074–2088.
- [76] Maria Valera and Sergio A Velastin. 2005. Intelligent distributed surveillance systems: A review. *IEE Proceedings-Vision, Image and Signal Processing* 152, 2 (2005), 192–204.
- [77] Harald J Van Heerde, Isaac M Dinner, and Scott A Neslin. 2019. Engaging the unengaged customer: The value of a retailer mobile app. *International Journal of Research in Marketing* 36, 3 (2019), 420–438.
- [78] Ashish Vaswani, Noam Shazeer, Niki Parmar, Jakob Uszkoreit, Llion Jones, Aidan N Gomez, Łukasz Kaiser, and Illia Polosukhin. 2017. Attention is all you need. In *Proceedings of the Annual Conference on Neural Information Processing Systems (NeurIPS)*.
- [79] Raghav H. Venkatnarayan and Muhammad Shahzad. 2019. Enhancing Indoor Inertial Odometry with WiFi. *Proceedings of the ACM on Interactive, Mobile, Wearable and Ubiquitous Technologies (IMWUT)* 3, 2, Article 47 (2019), 27 pages.
- [80] Quoc Duy Vo and Pradipta De. 2015. A survey of fingerprint-based outdoor localization. *IEEE Communications Surveys & Tutorials* 18, 1 (2015), 491–506.
- [81] Florian Walch, Caner Hazirbas, Laura Leal-Taixe, Torsten Sattler, Sebastian Hilsenbeck, and Daniel Cremers. 2017. Image-based localization using Istms for structured feature correlation. In *Proceeding of the International Conference on Computer Vision (ICCV)*. IEEE, 627–637.
- [82] He Wang, Souvik Sen, Ahmed Elgohary, Moustafa Farid, Moustafa Youssef, and Romit Roy Choudhury. 2012. No need to war-drive: Unsupervised indoor localization. In *Proceedings of the International Conference on Mobile Systems, Applications, and Services (MobiSys)*. 197–210.
- [83] Jingwen Wang, Martin Rünz, and Lourdes Agapito. 2021. DSP-SLAM: Object oriented SLAM with deep shape priors. In *Proceedings of the IEEE International Conference on 3D Vision (3DV)*. IEEE, 1362–1371.
- [84] Yue Wang and Justin M Solomon. 2019. Deep closest point: Learning representations for point cloud registration. In *Proceeding of the International Conference on Computer Vision (ICCV)*. IEEE, 3523–3532.
- [85] Atilla Wohllebe, Phyllis Dirrler, and Szilárd Podruzsik. 2020. Mobile apps in retail: determinants of consumer acceptance—a systematic review. (2020).
- [86] Yuan Wu, Hai-Bing Zhu, Qing-Xiu Du, and Shu-Ming Tang. 2019. A survey of the research status of pedestrian dead reckoning systems based on inertial sensors. *International Journal of Automation and Computing* 16 (2019), 65–83.
- [87] Hongwei Xie, Tao Gu, Xianping Tao, Haibo Ye, and Jian Lv. 2014. MaLoc: A practical magnetic fingerprinting approach to indoor localization using smartphones. In *Proceedings of the ACM International Joint Conference on Pervasive and Ubiquitous Computing (UbiComp)*. ACM New York, NY, USA,

243–253.

- [88] Heng Xu, Xin Robert Luo, John M Carroll, and Mary Beth Rosson. 2011. The personalization privacy paradox: An exploratory study of decision making process for location-aware marketing. *Decision support systems* 51, 1 (2011), 42–52.
- [89] Hang Yan, Sachini Herath, and Yasutaka Furukawa. 2020. RoNIN: Robust neural inertial navigation in the wild: Benchmark, evaluations, & new methods. In *Proceedings of the IEEE International Conference on Robotics and Automation (ICRA)*. IEEE.
- [90] Hang Yan, Qi Shan, and Yasutaka Furukawa. 2018. RIDI: Robust IMU double integration. In *Proceedings of the European Conference on Computer Vision (ECCV)*. Springer, 621–636.
- [91] Faheem Zafari, Athanasios Gkelias, and Kin K Leung. 2019. A survey of indoor localization systems and technologies. *IEEE Communications Surveys & Tutorials* 21, 3 (2019), 2568–2599.
- [92] Xiaopeng Zhao, Zhenlin An, Qingrui Pan, and Lei Yang. 2023. NeRF2: Neural radio-frequency radiance fields. In *Proceedings of the ACM Annual International Conference on Mobile Computing and Networking (MobiCom)*. ACM New York, NY, USA, New York, NY, USA, Article 27.
- [93] Heng Zhou and Takuya Maekawa. 2023. GPS-assisted Indoor Pedestrian Dead Reckoning. *Proceedings of the ACM on Interactive, Mobile, Wearable and Ubiquitous Technologies (IMWUT)* 6, 4 (2023), 1–36.